Applied Catalysis B: Environmental 121–122 (2012) 239–251

Contents lists available at SciVerse ScienceDirect

Applied Catalysis B: Environmental

journal homepage: www.elsevier.com/locate/apcatb

Coupled NO_x storage and reduction and selective catalytic reduction using dual-layer monolithic catalysts

Yi Liu, Michael P. Harold*, Dan Luss*

Department of Chemical & Biomolecular Engineering, University of Houston, 77204-4004, United States

ARTICLE INFO

Article history:
Received 9 January 2012
Received in revised form 3 April 2012
Accepted 9 April 2012
Available online 15 April 2012

Keywords:
Dual-layer catalyst
Monolith
Lean NO_x Trap
NO_x storage and reduction
Selective catalytic reduction
Ceria
Cu
Fe
ZSM-5
NH_3
Lean NO_x reduction
Pt

ABSTRACT

Lean reduction of NO_x (NO and NO_2) was studied using monolith-supported catalysts consisting of a layer of a metal-exchanged (Fe, Cu) zeolite (ZSM-5) selective catalytic reduction (SCR) catalyst deposited on top of a Pt/Rh/BaO/CeO_2 lean NO_x trap (LNT) catalyst. During periodic switching between lean and rich feeds, the LNT layer reduces NO_x to N_2 and NH_3. The SCR layer traps the latter, resulting in additional NO_x reduction. The dual-layer catalysts exhibited high N_2 selectivity and low NH_3 selectivity over the temperature range of 150–300 °C. The NO_x conversion was incomplete due to undesired side reactions in the LNT layer, such as NH_3 oxidation to N_2O at low temperature and NO_x at high temperature. The NO_x conversion and N_2 selectivity of the Cu-exchanged ZSM-5 was higher than that of the Fe-exchanged ZSM-5. This was due to a higher low temperature SCR activity and a higher NH_3 storage capacity on the Cu-zeolite. The dual-layer catalyst had a higher NO_x conversion than the LNT catalyst below 300 °C and a higher N_2 selectivity over the entire temperature range when H_2O and CO_2 were present in the feed. The NO_x storage capacity and NH_3 generation increased upon addition of CeO_2 to the LNT layer below 250 °C. It also led to increased NH_3 oxidation at high temperatures. The addition of ceria mitigated the undesirable migration of Pt between the LNT and SCR layers. Hydrothermal aging had a smaller effect on dual-layer catalysts containing ceria.

1. Introduction

Diesel and lean burn engines are well known for their high power output achieved with superior fuel economy and reduced CO_2 emissions compared to gasoline engines. However, one obstacle for wide adoption of lean burn engines is their failure to meet stringent emission regulations for NO and NO_2 (NO_x) using conventional after treatment technology such as the three-way catalytic converter (TWC). Two recently commercialized catalytic processes for lean NO_x reduction are NO_x storage and reduction (NSR) and selective catalytic reduction (SCR). The SCR process used commercially in stationary applications uses ammonia as a reductant. Relatively low cost metal-exchanged zeolite catalysts provide high activity, durability, and good sulfur tolerance. However, the high fixed cost of the urea feed system precludes the use of SCR for light-duty diesel-powered vehicles. In contrast, NSR is carried out over a lean NO_x trap (LNT) containing a more expensive precious metal catalyst and requires frequent periodic shifting between fuel-lean and fuel-rich modes. The fuel itself or its partially oxidized products (e.g. CO, H_2, low molecular weight olefins, etc.) serve as the reductants. Given the expense and inferior catalyst durability, LNT technology currently see application only in light-duty lean burn vehicles.

NSR is carried out by a periodic shift between, a lean storage phase and a rich regeneration phase on a multi-functional catalyst. NO_x generated from the fuel combustion is captured and stored on LNT catalysts in the presence of excess O_2 when the engine is operated in the conventional fuel-lean mode. At typical LNT space velocities (30,000–100,000 h^{-1}), the lean mode lasts for 1–2 min, following which the exhaust is switched to a much shorter, 3–20 s fuel-rich feed. This may be accomplished by injecting supplemental diesel fuel into the engine in order to consume the excess O_2, which produces a rich mixture of hydrocarbons, CO, and H_2 for the LNT regeneration. The primary reaction products are the desired N_2, CO_2, and H_2O as well as undesired NH_3 and N_2O.

In addition to platinum-group-metals (PGM; usually Pt or Pt/Rh), LNT catalyst contains NO_x adsorption materials such as BaO, supported on high surface area γ-Al_2O_3. Ceria (CeO_2) is often added to the LNT catalyst. Ji et al. [1] reported that the addition of ceria to the Ba-based LNT catalyst results in additional NO_x storage capacity and that the NO_x stored on CeO_2 can be reduced more easily due to the lower thermal stability of ceria-based nitrates. This has

* Corresponding authors. Tel.: +1 7137434307; fax: +1 7137434323.
E-mail addresses: mharold@uh.edu (M.P. Harold), dluss@uh.edu (D. Luss).

0926-3373/$ – see front matter © 2012 Elsevier B.V. All rights reserved.
http://dx.doi.org/10.1016/j.apcatb.2012.04.013

important implications at the low temperatures (<250 °C) encountered during start-up or low-load operation. Researchers at Honda suggested that in situ hydrogenation using H_2 generated by the ceria-promoted water-gas-shift (WGS) reaction provides complete and effective LNT regeneration [2,3]. In addition to providing NO_x storage sites and to enhancing WGS activity, ceria improves catalyst durability and sulfur resistance. Hatanaka et al. [4] reported that the interaction between oxidized Pt and ceria leads to the formation of nanocomposite oxides. The resulting Pt—O—Ce bond inhibits Pt sintering and helps keep the Pt in a well-dispersed state in an oxidizing environment. Kwak et al. [5] used ceria as a supporting material for Pt/BaO. No measureable Pt sintering or BaS formation was observed during desulfation up to 600 °C.

The presence of combustion products H_2O and CO_2 in the feed affects the LNT performance. H_2O decreases the NO oxidation rate but has only a minor effect on the cycle-average NO_x conversion. CO_2 leads to formation of $BaCO_3$, which has a higher thermal stability than either BaO or $Ba(OH)_2$, decreasing the NO_x conversion. Ren et al. [6] studied the impact of both H_2O and CO_2 on deNOx efficiency of LNT catalysts. Mulla et al. [7] reported that water vapor in the feed decreases the Pt active sites and thus inhibits NO oxidation to NO_2. Lietti et al. [8] proposed that water could promote NH_3 formation during the reduction of stored NO_x, while CO_2 strongly inhibits the reduction of nitrates by H_2 or NH_3. Frola et al. [9] used in situ surface FT-IR to analyze NO_x storage. They determined that CO_2 inhibits the nitrite formation and the subsequent nitrate formation. Lindholm et al. [10] investigated the influence of H_2O and CO_2 over different LNT catalysts. H_2O adsorption decreased the NO_x storage on alumina, while CO_2 inhibited the NO_x storage on barium. NH_3 formation was promoted by CO_2 at low temperatures.

The formation and role of byproduct ammonia during NSR is as important as it is complex, prompting a large number of studies. Nova et al. [11] proposed that NH_3 was a key intermediate for N_2 formation and could be produced in high selectivity when H_2 was used as the reductant. Mulla et al. [12] found that NH_3 was formed during the regeneration of stored NO_x, acting as an H-atom carrier. Wang et al. [13] investigated the effect of regeneration conditions on NH_3 formation under simulated diesel exhaust. The NH_3 selectivity increased with the steam reforming activity due to the generation of H_2. Lietti et al. [8] determined that the reaction of ammonia with nitrates was a major route for nitrogen formation. Clayton et al. [14] showed through the construction of spatial profiles of N-containing products that the reaction of H_2 with stored NO_x and the sequential NH_3 formation and reaction with downstream nitrate was a major route for N_2 formation. They identified favorable cyclic conditions for NH_3 formation; i.e. high H_2/NO_x, moderate temperature, and low Pt dispersion. [15] The temperature for maximum NH_3 production decreased with an increase in Pt dispersion. They attributed this trend to the rate limiting transport of stored NO_x to the Pt/BaO interface; i.e. transport limitations lead to a localized higher H_2/NO_x ratio that is favorable for NH_3 production. [16] Bhatia et al. [17] corroborated this NO_x regeneration mechanism in a follow-up modeling study. Luo and Epling [18] proposed an alternative mechanism in which H adatoms diffuse on the exposed alumina support. A recent modeling and experimental study of Shakya et al. [19] suggests that both stored NO_x and H diffusion may be involved in the regeneration.

SCR is the second major NO_x abatement technology for lean burn diesel vehicles, which involves the reaction between NH_3 and NO_x in the presence of excess O_2. Used in stationary applications and heavy-duty vehicles, it requires injection of NH_3 or of its precursor urea where it mixes with NO_x and O_2. While the urea–SCR system has lower catalyst cost than the PGM-containing LNT system, the use of urea leads to problems, such as urea fouling and NH_3 slip [20,21]. Another option is the use of reductants to react with NO_x stored in the LNT to produce NH_3. The gas mixture fed to the SCR reactor undergoes the following global reactions:

$$\text{StandardSCR}: 4NO + 4NH_3 + O_2 \Leftrightarrow 4N_2 + 6H_2O \quad (R1)$$

$$\text{FastSCR}: NO + NO_2 + 2NH_3 \Leftrightarrow 2N_2 + 3H_2O \quad (R2)$$

$$NO_2\text{SCR}: 6NO_2 + 8NH_3 \Leftrightarrow 7N_2 + 12H_2O \quad (R3)$$

Fe- and Cu-exchanged zeolites are commonly used as NH_3—SCR catalysts following considerable research. Colombo et al. [22] reported that a Cu-based zeolite had a higher NH_3 storage capacity than a comparable Fe-based zeolite. It also had a higher catalytic activity for the standard SCR and ammonia oxidation reactions, as well as a lower sensitivity to NO_2/NO_x feed ratio. Fedeyko et al. [23] measured the catalytic behavior of the Fe/Cu zeolites via FT-IR spectroscopy and found that NH_3 has a stronger site blocking effect on the Fe-zeolite than on the Cu zeolite. Metkar et al. [24] found that the standard SCR rate on Fe-ZSM-5 exhibited a slightly negative order with respect to NH_3. Kamasamudram et al. [25] applied a four-step experimental protocol to assess the catalytic functions of different SCR catalysts. The differences between the Cu- and Fe-zeolites transient behaviors during low temperature are related to differences in their NH_3 coverage-dependent adsorption. Cu-zeolite is less sensitive to the NO_2/NO_x ratio and is more active at low temperatures when the ammonia coverage is high [26]. Metkar et al. [27] compared the NO_x reduction by three Fe-zeolite and Cu-zeolite combined configurations as “sequential brick”, “mixed washcoat” and “dual-layer”. The NO_x reduction efficiency of a dual-layer catalyst with Fe-zeolite on top of Cu-zeolite is comparable to that obtained from sequential bricks. Washcoat diffusion limitations for the former favor the dual-layer Fe/Cu configuration.

Active research efforts aim to determine a catalyst architecture that will avoid the need for a urea feed system, but which achieves the required NO_x reduction while minimizing the amount of expensive PGM in the LNT. The approach involves the combination of NSR and LNT, referred to as LNT/SCR technology. Several LNT/SCR configurations or architectures were proposed in patents by Ford (Gandhi et al. [28,29]). One approach is a sequential dual-brick LNT/SCR in which the upstream LNT catalyst brick is used to store NO_x and to reduce NO_x to a mixture of N_2 and NH_3, followed by a SCR catalyst brick that utilizes the generated NH_3 to reduce the unreacted NO_x that escapes from the LNT [30]. This system is similar to the conventional LNT in terms of the operating strategy but circumvents the need for a urea feed. Daimler AG commercialized a DOC–LNT–DPF–SCR aftertreatment system to meet US tier 2 bin 8 NO_x emission standard for a 3.0 L diesel engine [31]. Their study showed that low NO_x emission for US tier 2 bin 5 could be achieved by reducing the oxygen storage components in the LNT catalysts [32]. Eaton Inc. applied a similar configuration to reduce NO_x emission from heavy-duty diesel vehicles [33]. These results indicate that a dual brick LNT/SCR configuration enables NO_x abatement of both light- and heavy-duty diesel vehicles.

A variant of the LNT–SCR dual-brick configuration is the LNT–SCR multi-brick system proposed by Gandhi et al. [28] and investigated by Ford researchers. Theis et al. [34] showed that this architecture could reduce the PGM loading on the LNT catalysts by up to 50% and achieve the same NO_x conversion. These findings have motivated new research efforts to gain a better understanding of the behavior of LNT–SCR series configuration. Lindholm et al. [35] conducted experiments using a dual catalytic bed system comprising a $Pt/Ba/Al_2O_3$ LNT catalyst followed by a Fe-beta SCR catalyst. The combined system performance was superior to that of the single LNT catalyst at all temperatures. Pereda-Ayo et al. [36] studied a similar configuration with Fe-zeolite Beta downstream of $Pt/Ba/Al_2O_3$. They achieved NO_x removal efficiency and N_2 selectivity as high as 98% and 97%, respectively, using 3% H_2 during the LNT regeneration at 300 °C. Seo et al. [37] determined that

the optimal LNT to SCR volume ratio with regard to catalyst cost and NH_3 slip was 1:1. They also compared the deNOx performance of a LNT–SCR series configuration to that of a single LNT catalyst following hydrothermal aging and sulfur poisoning. NO_x conversion from the combined system was 10–30% higher than that of the LNT catalyst [38]. Bonzi et al. [39] studied both the double-bed and mixture architecture of $Pt/Ba/Al_2O_3$ LNT catalyst and Fe/ZSM5 SCR catalysts. Forzatti and Lietti [40] proposed a two-step in-series pathway to explain the temporal evolution of N_2. The first step is the formation of ammonia via a reaction of NO_x with H_2 and the second is the reaction between the so-formed ammonia and stored NO_x. With the second step identified as the rate-determining step, the downstream or mixed SCR catalyst can reduce NH_3 slip for NO_x elimination. Castoldi et al. [41] found that the presence of H_2O and CO_2 in the dual-bed and mixed LNT–SCR catalysts lowers the NO_x storage due to $BaCO_3$ formation, but improves N_2 selectivity during NH_3 oxidation on the LNT. Corbos et al. [42] studied the NO_x abatement over different mixtures of LNT and SCR catalysts. The physical mixture of $Pt\text{-}Rh/Ba/Al_2O_3$ and Cu/ZSM5 had the highest activity regardless of the reductants, reduction time and the presence of H_2O.

A dual-layer architecture is a potential alternative to the sequence of LNT–SCR bricks. Nakatsuji and co-workers from Honda [43] proposed a catalyst system comprising a solid acid (Bronsted acid–based zeolite) on top of Pt/OSC (oxygen storage catalyst). NO_x is stored on the OSC function during the lean phase, while NH_3 forms by the stored NO_x. NH_3 is stored on the solid acid function during the rich feed. During the lean feed, NO_x is partially reduced by the adsorbed NH_3. Honda reported the use of a SCR-on top of Pt/OSC composite to meet NO_x emission standards of US tier 2 bin 5 [2,3]. While Honda's work provoked interest in this approach, it did not provide sufficient information about the catalyst or understanding of the fundamental workings of the LNT–SCR dual-layer catalyst.

In this study, dual-layer monolith catalysts comprising a SCR layer deposited on-top of a LNT layer was prepared and tested. We investigate the impacts of the SCR catalyst type (Fe-, Cu-), H_2O and CO_2 addition, LNT ceria loading, and temperature on the cycle-averaged NO_x conversion and product distribution. Finally, the effects of aging on the catalyst performance are examined. The findings are interpreted in terms of the individual performance features of the LNT and SCR catalysts. This is the first fundamental study to provide insight and understanding of the dynamic performance of a dual-layer LNT–SCR. This information is essential for any attempt to minimize the amount of required expensive PGM. Moreover, the results enable a comparison of the performance of dual-layer architecture with the sequential architecture.

2. Experimental

2.1. Catalyst preparation and characterization

Model LNT catalysts were supplied by BASF Catalysts (Iselin, NJ). Cylindrical cores (diameter = 1.9 cm, length = 7.6 cm) were cut into smaller monolithic cores (28 channels; D = 0.8 cm, L = 2.0 cm). The washcoat loading on the cordierite structure (~62 channels/cm^2) catalysts was ca. 4.6 g/in^3 and contained Pt/Rh, and different amounts of storage components BaO and CeO_2. The compositions of the three catalysts, labeled as LNT1, LNT2 and LNT3, are reported in Table 1.

Fe/ZSM5 catalyst powder was provided by Sud-Chemie (Munich, Germany). We synthesized Cu/ZSM5 catalyst powder by the following wet-ion exchange method [24,27]. NH_4/ZSM5 powder having a Si/Al ratio of 23 was acquired from Zeolyst (PA, USA). A protonated powder (H/ZSM5) was obtained by calcining NH_4/ZSM5 at 550 °C for 5 h. The H/ZSM5 was converted to Na/ZSM5 by dispersing the catalyst powder in 0.1 M $NaNO_3$ (Sigma–Aldrich) solution. The ion exchange was conducted for 24 h with continuous stirring at ambient temperature and neutral pH (~7). The powder was obtained following filtration and washing in a centrifuge (Avanti® J-E BioSafe, Beckman Coulter) and drying overnight at 120 °C. The Na^+ exchange and drying were repeated twice to maximize the exchange ratio. The Na/ZSM5 powder was obtained after calcination at 550 °C for 5 h. The Cu/ZSM5 was prepared by contacting Na/ZSM5 with a 0.02 M copper acetate (Sigma–Aldrich) solution, which was continuously stirred for 24 h at ambient temperature. The solution pH was adjusted to ~6 by 0.1 M acetic acid solution. The Cu^{2+}/Al^{3+} ratio was in range of 0.5–1. The ion-exchange procedure was repeated three times. Finally, the Cu/ZSM5 was obtained by calcining the powder at 550 °C for 5 h.

Table 1
Properties of LNT catalysts.

	LNT1	LNT2	LNT3
PGM (g/ft^3)	90	90	90
Ba (wt%)	14	14	14
Ce (wt%)	0	17	34

Details of the washcoating procedure were described by Metkar et al. [24,27]. An aqueous slurry comprising of 32 wt% catalyst powder, 8 wt% boehmite and balance water was ball-milled for 24 h to obtain catalyst particles with a size in the range of 1–5 μm. The slurry pH was adjusted to ~6 by adding 0.1 M acetic acid before washcoating. The SCR monolith was prepared by dip-coating an empty monolith in the slurry for 30 s from each end. The excess slurry was cleared by feeding compressed air sequentially into both ends for 10 s. The washcoated monolith was then dried at 120 °C overnight. The washcoating was repeated until the desired loading was obtained. The final step involved the calcination of the monolithic catalyst at a temperature ramp of 23 °C/h and then holding it at 550 °C for 5 h. The typical loading of the monolith washcoat after calcination was in the range of 0.8–1.0 g/in^3. The same dip-coating procedure was used to prepare the mixed washcoat LNT–SCR monolithic catalysts having a washcoat loading of about 3.0 g/in^3 (LNT: 2.1 g/in^3; SCR: 0.9 g/in^3). The dual-layer monoliths were prepared by depositing a SCR layer on top of the LNT bottom layer. The LNT monolith was calcined at 550 °C for 5 h before washcoating to avoid barium leaching.

The SCR loading was approximately 0.9 g/in^3 in all the dual-layer catalysts. A schematic of a SCR–LNT dual-layer catalyst is shown in Fig. 1a. The images of LNT catalysts before and after SCR washcoating are shown in Fig. 1b. As can be seen, the LNT layer has a non-uniform thickness due to the thicker loading in the corners. The washcoat thickness of the monolith channel was measured with a scanning electron microscope (SEM; JEOL JSM-6330F). The thinnest peripheral average of the LNT layer is about 60–80 μm and the maximum thickness is about 260–290 μm at the corners. After washcoating, a uniform layer of SCR catalyst (thickness of 40–50 μm) was deposited on top of the LNT layer. We refer to this catalyst as a dual-layer LNT–SCR.

The Pt, Rh, Ba, Ce, Cu, Fe, Si, Al and O concentrations in the dual-layer catalysts were measured using energy dispersive spectroscopy (EDX/EDS). To study the interlayer mixing, both fresh and aged dual-layer catalysts were analyzed by SEM–EDS. Hydrothermal aging was accomplished by calcining the fresh dual-layer catalyst at 600 °C in air for 100 h.

2.2. Reactor experiment

The bench-scale reactor set-up has been used in several previous studies described elsewhere [14–16,44,45]. Gas flow rates

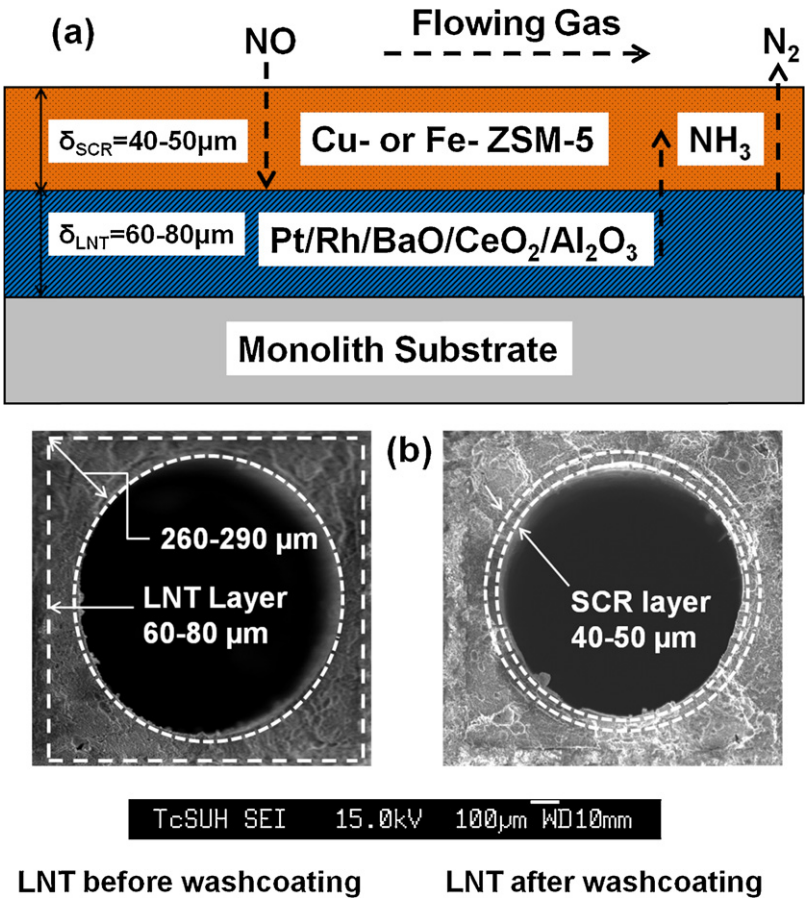

Fig. 1. (a) Schematic of a dual-layer catalyst; (b) cross-section SEM micrographs of LNT1 catalyst before and after SCR washcoating.

were controlled by a series of mass flow controllers (MKS Inc.) before entering the inline static mixers while water was fed by a syringe pump (ISCO Model 500D) and vaporized in the heated line. A switching valve upstream of the reactor controlled the feed streams. The monolith was wrapped by Fiberfrax® ceramic paper and positioned in a quartz tube flow reactor (1.2 cm diameter, 40.6 cm length; Technical Glass Products), placed inside a tube furnace (Mellen M300) that controlled the catalyst temperature. The effluents were monitored by a FT-IR (Thermo Nicolet Nexus 470) and a quadrupole mass spectrometer (QMS; Cirrus LM99, MKS Inc.). The concentrations of NO, NO_2, N_2O, NH_3, CO, CO_2 and H_2O were measured by the FT-IR. The H_2, O_2 and N_2 concentrations were monitored by the QMS. Both instruments were calibrated daily before the start of the experiments. When the feed did not contain CO_2, the nitrogen balance closed within 5%. When the feed contained CO_2, the amount of N_2 formed was obtained by an overall nitrogen balance due to the overlap with CO of the $m/e = 28$ in the QMS. The effluent flow time lags between the reactor and FTIR and the reactor and QMS were determined by replacing the reactor with an unloaded quartz tube. Two 0.5 mm type-K stainless steel sheathed thermocouples (Omega Inc.) measured the temperature. One placed 0.5 cm upstream of the monolith measured the feed temperature and the second placed in the middle of the center channel of the monolith measured the catalyst temperature.

A cycle consisted of a periodic shift between the lean and rich feeds. Unless otherwise stated, the lean feed, containing 500 ppm NO and 5% O_2 in Ar was fed for 60 s. It was followed by a rich feed containing 2.5% H_2 in Ar for 5 s. In selected experiments (Section 3.2) both CO_2 (2%) and H_2O (2.5%) were added. The cycle average H_2:NO feed ratio was 1.04 times higher than the stoichiometric ratio needed for NH_3 formation:

$$16H_2 + 4NO + 3O_2 \rightarrow 4NH_3 + 10H_2O \quad \text{(R4)}$$

The total flow rate was 1000 sccm (GHSV = 60,000 h^{-1}, calculated based on total monolith volume and standard temperature and pressure). It took approximately 10 min to reach a periodic state while at least 50 cycles were run at each temperature. The final ten cycles were averaged to determine the cycle-averaged NO conversion and product selectivity for a particular operating condition. The feed temperature was increased from 100 to 400 °C in steps of 50 °C. At each temperature, cycle-averaged quantities were determined. The NO conversion was calculated by

$$X_{NO} = 1 - \frac{\int_0^{\tau_s} F_{NO}(t)dt}{\int_0^{\tau_1} F_{NO}^i(t)dt} \quad (1)$$

When large amount of NO_2 was present, the NO_x conversion was calculated by

$$X_{NO_X} = 1 - \frac{\int_0^{\tau_s} [F_{NO}(t) + F_{NO_2}(t)]dt}{\int_0^{\tau_1} F_{NO}^i(t)dt} = X_{NO} - \frac{\int_0^{\tau_s} F_{NO_2}(t)dt}{\int_0^{\tau_1} F_{NO}^i(t)dt} \quad (2)$$

The NH_3 and NO_2 selectivity were calculated by

$$S_i = \frac{\int_0^{\tau_s} F_i(t)dt}{\int_0^{\tau_1} F_{NO}^i dt - \int_0^{\tau_s} F_{NO}(t)dt} \quad i = NH_3, \quad NO_2 \quad (3)$$

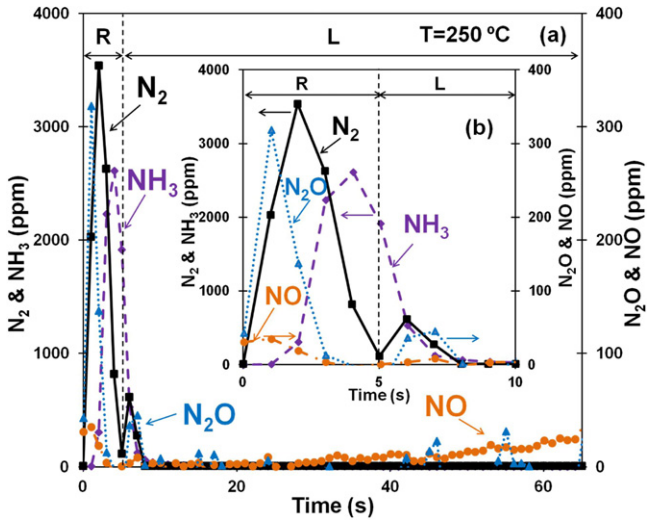

Fig. 2. (a) Effluent for Pt/Rh/BaO LNT1 catalyst over a time period of 0–65 s; (b) Insert shows effluent over 0–10 s.

and the N_2 and N_2O selectivity were calculated by

$$S_i = \frac{\int_0^{\tau_s} 2 * F_{N_2/N_2O}(t)dt}{\int_0^{\tau_1} F_{NO}^{i}dt - \int_0^{\tau_s} F_{NO}(t)dt} \quad i = N_2, \quad N_2O \tag{4}$$

Here τ_1 and τ_s are the duration of lean phase feed and a lean-rich total cycle (s). F_{NO}^{i} is the NO feed rate and $F_{NO}(t)$, $F_{NH_3}(t)$, $F_{NO_2}(t)$, $F_{N_2O}(t)$, $F_{N_2}(t)$ the corresponding effluent molar flow rates (mole/s).

A series of steady state experiments was conducted to evaluate the catalyst properties. The total flow rate was 1000 sccm in all the experiments. The standard SCR reaction was used to assess the activity of the FeZ and CuZ SCR, both of which have the same loading of 0.9 g/in^3. The feed contained 500 ppm NO, 500 ppm NH_3, and 5% O_2 in Ar. During the NH_3 and NO_2 storage experiments, 500 ppm NH_3 or NO_2 was fed to the catalyst for 20 min. The total NH_3 or NO_x uptake was calculated by subtracting the effluent amount from that fed. The physisorbed species were swept by a 10-min Ar purge. After that, the monolith temperature was increased by a temperature ramp of 20 °C/min to 450 °C in Ar. The amount of NH_3 or NO_x released was referred to as chemisorbed species. The nitrogen balance was closed by comparing the sum of physisorbed and chemisorbed species with the total feed amount. The balance closed within 5%. NH_3 oxidation was carried out with a feed gas containing 500 ppm NH_3 and 5% O_2 in Ar to quantify the rate of this important side reaction. The reaction order of NH_3 oxidation was determined from experiments in which the NH_3 concentration varied from 200 to 1000 ppm. The total flow rate was decreased to 500 sccm and the O_2 concentration was fixed at 5%. The NH_3 conversion was less than 15% at 150 °C. The apparent reaction rate was calculated by

$$\gamma_{NH_3} = \frac{F_{in}X_{NH_3}}{m_{w.c.}} \tag{5}$$

where F_{in} is the feed rate of NH_3 (mole/s), X_{NH_3} the NH_3 conversion (%) and $m_{w.c.}$ the washcoat mass (g).

3. Results and discussion

3.1. Comparison of effluents from LNT and dual-layer catalysts

Fig. 2a shows typical temporal effluent concentration from the Pt/Rh/BaO/Al_2O_3 LNT catalyst (LNT1) during a 60 s lean-5 s rich cycle at a feed temperature of 250 °C. The inset Fig. 2b describes the effluent during the 5 s rich regeneration and subsequent five seconds of lean feed. The temporal effluent is characteristic of a LNT regeneration using H_2 as the reductant. A NO release peak ("NO spike" or "NO puff") appeared at the beginning of the rich feed. Nearly coincident with the NO spike was N_2O evolution. N_2 and NH_3 appeared consecutively with some overlap. For this operating condition, the maximum N_2 and NH_3 effluent concentrations were 3550 ppm and 2610 ppm, respectively. By integrating the areas under the effluent graphs, the computed NH_3 yield (6.1 μmole) is comparable to that of N_2 (7.8 μmole). The rather large amount of generated NH_3 points out the potential for a dual-layer catalyst application. That is, by adding a top-layer of SCR catalyst, the slipping NH_3 could be captured and converted selectively to N_2 by the standard SCR reaction between NH_3, NO, and O_2. The decrease of the NH_3 slip increases the NO conversion. We return to this concept below.

The data in Fig. 2 show that a second pair of N_2 and N_2O peaks formed during the lean feed. These were followed by a nearly 30-s period in which no species containing N were measured, indicating that NO oxidation and NO_x storage were the main processes that occurred during the remainder of the lean feed. About 35 s after the shift to a lean feed, some NO emerged. Its concentration gradually increased during the remainder of the lean feed, due to the expected saturation of the NO_x storage sites. No NO_2 was observed under these conditions.

The species evolution from the LNT1 catalyst agrees with reports by other investigators. The occurrence of the NO_x spike at the beginning of the rich feed is an important feature of LNT regeneration [1,14–16,46]. Ji et al. [1,46] attributed its formation to the rate of NO_x reduction being slower than that of nitrate decomposition. The sequential appearance of N_2O, N_2, and NH_3 is also a common feature. At the beginning of the regeneration the conditions are more favorable for N_2O production; i.e. a relatively high local NO/H ratio. As the regeneration proceeds, deeper reduction (decreasing NO/H ratio) favors NH_3 formation. The NH_3 produced upstream travels downstream and reacts with stored NO_x, producing N_2, as reported among others by Mulla et al. [7], Ji et al. [1], Lietti et al. [8], and Clayton et al. [14–16]. The small N_2 and N_2O peaks at the beginning of the lean feed are attributed to the oxidation of NH_3. Clayton et al. [15] speculated that the oxidation of accumulated NHx species from the previous rich feed is responsible for N_2 formation during the subsequent lean feed.

Fig. 3 compares the performance of the Pt/Rh/BaO/Al_2O_3 LNT1 catalyst (Fig. 3a) to the dual layer CuZ/LNT1 (Fig. 3b) and FeZ/LNT1 catalysts. Each plot compares the cycle-averaged NO conversion and product selectivities as a function of feed temperature between 100 and 400 °C. The black line and points describe the NO conversion and the shaded/colored bars the product selectivities. For each catalyst the NO conversion and N_2 selectivity increased monotonically with feed temperature, while the N_2O selectivity decreased (except for the FeZ/LNT1 which had a slight maximum). Using the LNT1 catalyst, the maximum NH_3 selectivity was about 40% at 150 °C. A large amount of NH_3 was produced in the temperature range of 150–300 °C. These trends are consistent with reported results by previous studies (e.g. [47]).

It is important to select a SCR catalyst suitable for the dual-layer application. The SCR layer is exposed to a range of NH_3 and NO/NO_2 concentrations along the monolith channels due to reactions in the underlying LNT layer. The dependence of the NO_x conversion and NH_3 selectivity on the temperature is evidence for this fact (Fig. 3a). (Remark: although trace amounts of NO_2 were detected in the experiments shown in Fig. 3a, much more NO_2 was detected in the presence of H_2O and CO_2 as we report later.) The ability of the zeolitic function of the SCR catalyst to adsorb NH_3 is essential for additional NO_x reduction. The SCR layer activity should be high and minimally inhibited by the adsorbed NH_3. For this reason, we tested the performance of two dual-layer catalysts, one

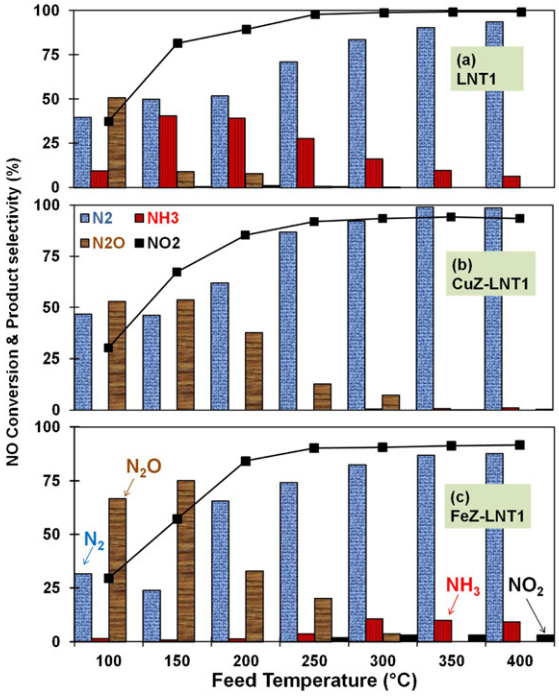

Fig. 3. Time averaged performance of (a) LNT1 catalyst; (b) CuZ–LNT1 multilayer catalyst; (c) FeZ–LNT1 multilayer catalyst. The black curves with square points are the NO conversion and the color bars are the product selectivities. The same format is used in other similar figures. (For interpretation of the references to color in this figure legend, the reader is referred to the web version of the article.)

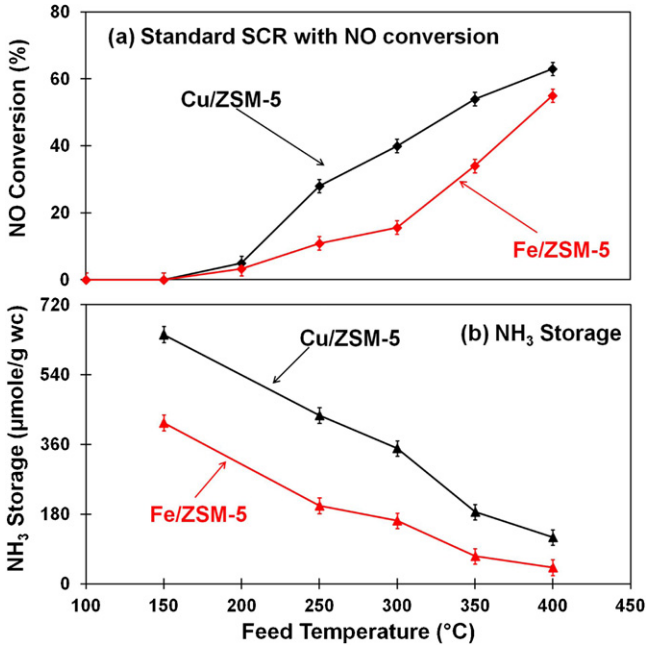

Fig. 4. (a) NO conversion and (b) NH_3 storage capacity on Fe- (black lines) and Cu-ZSM-5 (red lines) samples. (For interpretation of the references to color in this figure legend, the reader is referred to the web version of the article.)

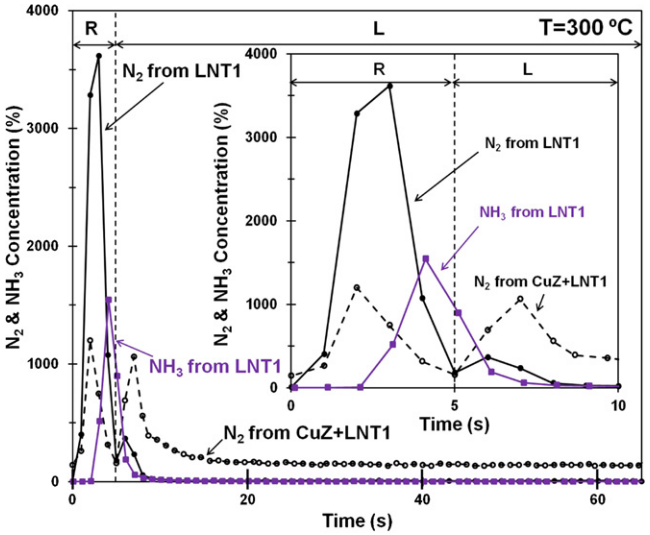

Fig. 5. Comparison of N_2 and NH_3 effluent from LNT1 and CuZ–LNT1 catalysts.

containing Fe-exchanged ZSM-5 and the other Cu-exchanged ZSM-5, coated on top of the same LNT base layer. Both zeolitic layers had the same loading and were exposed to the same cyclic feed; i.e. 60 s lean, 5 s rich. Fig. 3b shows the dependence of the NO conversion and product selectivity of the CuZ/LNT1 dual-layer catalyst on the feed temperature. Similar to the LNT1 layer alone (Fig. 3a), the NO conversion and N_2 selectivity increase monotonically with feed temperature. On the other hand, the NH_3 produced by the LNT was completely converted. An additional effect of the Cu-zeolite layer is a moderate increase in N_2O for feed temperatures lower than 250 °C. These trends are explained below. Fig. 3c shows the NO conversion and product selectivity of the FeZ/LNT1 dual-layer catalyst. The NO conversion and N_2 selectivity for both the LNT1 and CuZ/LNT1 increased with the feed temperature, while the N_2O selectivity generally decreased. However, the FeZ/LNT1 catalyst had some NH_3 slip, a higher N_2O selectivity, and a somewhat lower NO conversion and N_2 selectivity over the entire LNT1 and CuZ/LNT1 temperature range.

In order to examine differences between the two SCR zeolite catalysts, we compared their respective NH_3 storage and SCR activities. Fig. 4 compares the temperature dependencies; i.e. 20-min NH_3 storage capacity and NO conversion for a standard SCR feed (containing NO, O_2, and NH_3) for both Cu/ZSM5 and Fe/ZSM5. The trends same as those reported by previous studies [22–27]. The NO conversions are somewhat lower than those obtained by Metkar et al. on similar catalysts [27]; the difference is attributed to a somewhat lower washcoat loading in the current study (9 wt% vs. 11 wt%) and to the use of centrifugation rather than filtration during the catalyst synthesis. The NH_3 storage capacity and NO conversion of the FeZ catalyst are lower than that of the CuZ catalyst over the entire temperature range. These data show that the Cu zeolite performance is superior to that of the Fe zeolite. The CuZ catalyst adsorbed more NH_3 and its SCR activity was higher. Hence, the Cu/ZSM5 was used as the SCR catalyst in the remainder our study.

The rather high N_2O selectivity from the two dual-layer catalysts for temperatures below 250 °C suggests that the N_2O dissociation and reaction with stored NH_3 over the SCR catalysts is negligible. This is due to the limited catalytic activity at low temperatures. Su et al. [48] reported the N_2O dissociation to N_2 over a Fe/ZSM-5 commences above 400 °C and the presence of oxygen inhibits N_2O dissociation. N_2O dissociation over Cu/ZSM-5 only starts above 400 °C, as described by Groothaert et al. [49] Zhang et al. [50] investigated the reduction of N_2O by NH_3 and O_2 over a Fe-MOR zeolite catalyst. The reaction occurs at temperatures exceeding 350 °C. Hence, the N_2O produced from dual-layer catalyst is not likely to dissociate or react with the stored NH_3 over SCR catalysts. The source of the N_2O is discussed later.

Fig. 5 compares the transient N_2 and NH_3 concentrations from the LNT1 and dual-layer CuZ/LNT1 catalysts under the same operating conditions and illustrates the advantages of the dual-layer

catalyst concept. The behavior of the LNT1 catalyst at 300 °C is similar to that at lower temperature (e.g. 250 °C, Fig. 2). At 300 °C a large N_2 peak of 3600 ppm is immediately followed by a NH_3 peak of 1550 ppm. A second smaller N_2 peak of 370 ppm appears at the beginning of the lean phase. The most notable impact of coating the LNT1 catalyst with a layer of Cu/ZSM5 is the elimination of the NH_3 slip. In addition, the N_2 emission is more uniformly distributed over the rich and lean phases of the cycle. For example, during the rich phase, the N_2 peak is 1200 ppm for the CuZ/LNT1 catalyst, compared to 3600 ppm for the LNT1 catalyst. At the beginning of the lean phase, a N_2 peak of 1100 ppm appeared, of comparable magnitude to that during the rich stage. It was followed by a much lower, nearly constant but non-zero level of N_2 formation during the remainder of the lean phase. In comparison, the LNT1 catalyst generated a much smaller N_2 peak (350 ppm) during the lean feed. The SCR top-layer clearly modified the temporal effluent concentrations. The data suggests that NH_3 generated during the rich phase in the LNT layer is captured by the top SCR layer. Since the rich gas does not contain NO or O_2, no N_2 could be produced from the SCR catalyst. The stored NH_3 reacts with NO and O_2 fed during the subsequent lean phase. The N_2 peak at the beginning of the lean feed is an indication of NH_3 oxidation. NH_3 generated by the LNT1 catalyst during the rich step is trapped on the CuZ catalyst and then reacts with NO and O_2 during the lean phase. The maximum concentration of N_2 that can be produced at steady-state by the standard and fast SCR reactions (R1) and (R2) is 500 ppm, the stoichiometry being $NO_x/NH_3 = 1$. Thus, the NH_3 oxidation accounts for the additional N_2 in the lean N_2 peak, which is over 1000 ppm. During the remainder of the lean phase, the continuous N_2 production is evidence for the SCR reactions (R1)–(R3). The sustained evolution of N_2 from the dual-layer catalyst at a rather low concentration (150–160 ppm) is likely a result of slow ammonia desorption and diffusion from the zeolite layer.

The NH_3 formation and consumption profiles obtained using the dual-layer catalysts clearly differ from those obtained with the LNT catalyst. NH_3 is an important intermediate during the regeneration of stored NO_x in LNT catalysts, as reported by Mulla et al. [7], Lietti et al. [8,39,40] and Clayton et al. [14–16]. Its conversion to N_2 occurs by reaction with the downstream stored NO_x. The reaction rate depends on several factors, including the temperature, and the presence of H_2, among other factors. In contract, NH_3 generated in the LNT layer of the dual-layer catalyst diffuses into the adjacent zeolite layer where it can be adsorbed on the Cu and Bronsted acid sites. SCR reactions between the NH_3 and $NO/NO_2/O_2$ produce N_2 as the main product and N_2O as a byproduct. During the rich phase, the NH_3 adsorption leads to its disappearance as well as to the decrease of the N_2 peak (Fig. 5). During the lean phase, stored NH_3 is consumed by the SCR and NH_3 oxidation reactions. Undesired NH_3 oxidation increases the N_2 peak during the lean feed. It is undesired since ammonia is needed for NO_x reduction. This agrees with results reported by Nakatsuji et al. [43].

The NO_x conversion achieved by the dual-layer catalyst can be lower than that achieved by the LNT catalyst alone, as shown in Fig. 6a. This is a new, unexpected finding and does not agree with previously published results using other LNT/SCR configurations [28–45]. This counterintuitive trend results from an interaction between the two layers, and the reasons for the lower conversion are different for low and high temperature operation.

Fig. 4 shows that at temperatures below 250 °C the Cu/ZSM5 steady-state activity for standard SCR reaction is rather low. However, the zeolite still can store NH_3 produced in the LNT layer. In addition to the desired conventional SCR reactions (R1–R3) occurring on the SCR catalyst, which generate N_2, stored NH_3 may be consumed by the following competing reactions (R5–R9):

$$2NH_3 + 2NO_2 \rightarrow N_2 + NH_4NO_3 + H_2O \quad \text{(R5)}$$

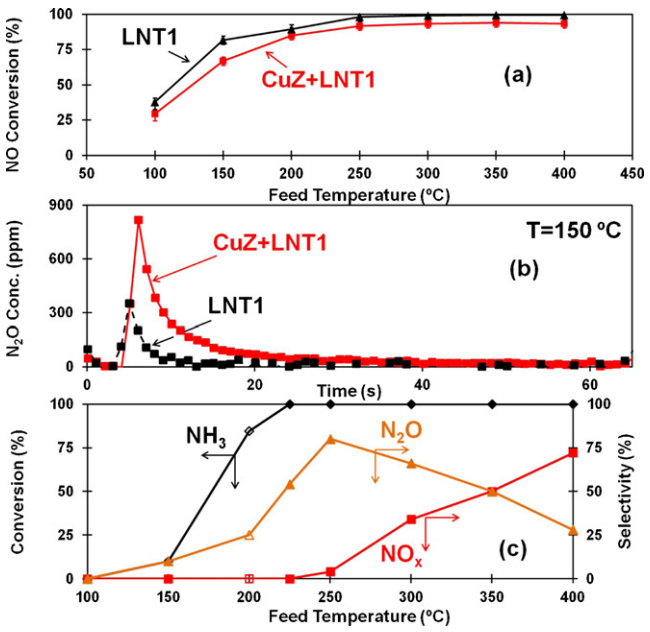

Fig. 6. (a) Comparison of NO conversion between LNT1 and multilayer catalyst; (b) Comparison of N_2O effluent from LNT and multilayer catalyst; (c) NH_3 oxidation to NO_x on LNT1 (the unfilled symbol denotes the result from the unsteady state).

$$NH_4NO_3 \rightarrow N_2O + 2H_2O \quad \text{(R6)}$$

$$NH_3 + Pt \rightarrow NH_3\text{–}Pt \quad \text{(R7)}$$

$$O_2 + 2Pt \rightarrow 2O\text{–}Pt \quad \text{(R8)}$$

$$NH_3\text{–}Pt + 2O\text{–}Pt \rightarrow 0.5\,N_2O + 1.5H_2O + 3Pt \quad \text{(R9)}$$

Fig. 6b compares the N_2O effluent concentration for both the LNT1 and dual-layer CuZ/LNT1 catalysts at 150 °C. The dual-layer catalyst generates more N_2O than the LNT catalyst during the lean phase. The N_2O may be formed by either one or both of two possible pathways. Reactions (R5) and (R6) comprise the formation and decomposition of NH_4NO_3. However, this pathway is not likely to occur to an appreciable extent because (i) it requires formation of NO_2, and NO oxidation is rather slow at 150 °C on these catalysts [44], and (ii) NH_4NO_3 decomposition is slow below 250 °C [51]. The second more viable route represented by steps (R7)–(R9) involves the adsorption and oxidation of NH_3 on the Pt crystallites of the LNT catalyst. The formation of N_2O during Pt-catalyzed NH_3 oxidation is well established [15,52,53]. Fig. 6c reports the NH_3 conversion and NO_x ($NO + NO_2$) and N_2O selectivities during NH_3 oxidation over the same LNT1 catalyst. The NH_3 conversion is over 80% at 200 °C and the N_2O selectivity is about 25%. These increase to 100% and 75%, respectively, by 250 °C. Fig. 7 reports the measured reaction rates for NH_3 oxidation over the three LNT catalysts at 150 °C. The positive dependence of the reaction rate on NH_3 concentration suggests that NH_3 trapped in the SCR layer diffuses to the underlying LNT layer where it is readily oxidized. This promotes NH_3 oxidation to N_2O at low temperatures.

At temperatures exceeding 250 °C, NO conversion by the dual-layer catalyst is still slightly lower than that by the LNT catalyst. At these temperatures, complete NH_3 conversion is obtained with increasing NO_x selectivity (Fig. 6c). The increase in the NO_x selectivity with temperature is a result of the consumption of NH_3. The NH_3 that is trapped likely intensifies the NH_3 oxidation to NO_x on the Pt, resulting in a lower NO conversion.

In order to assess the importance of segregating the NSR and SCR functions (as separate layers), experiments were conducted in which a mixture of LNT and SCR catalysts was deposited on the washcoat and its performance tested. The LNT catalyst powder was

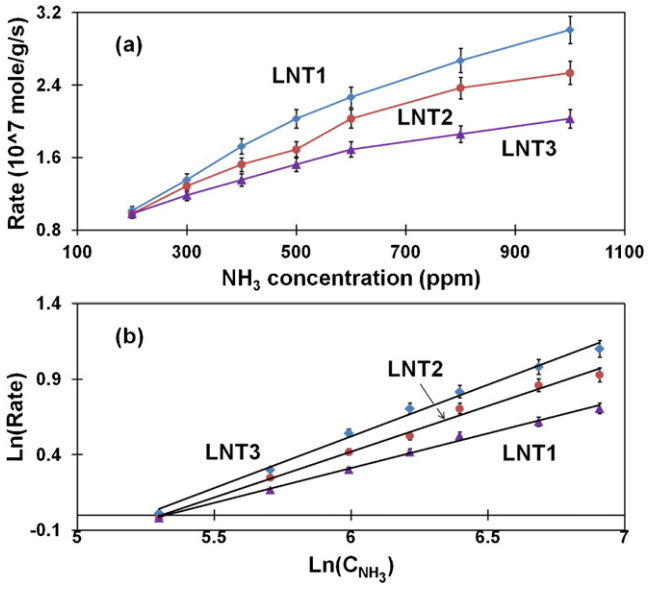

Fig. 7. The apparent reaction order of NH_3 during NH_3 oxidation at a feed rate of 500 ppm and 5% O_2 at 150 °C over three LNT catalysts. Part (b) is the logarithm plot of part (a). For LNT1, $y = 0.460x–2.449$, $R^2 = 0.9957$; for LNT2, $y = 0.607x–3.2178$, $R^2 = 0.9922$; for LNT3, $y = 0.684x–3.5823$, $R^2 = 0.9935$.

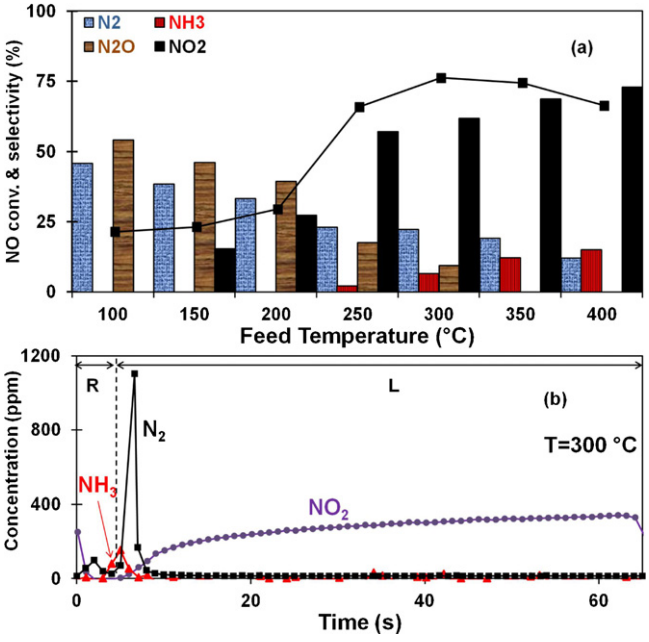

Fig. 8. (a) Performance of LNT1–CuZ mixed washcoat catalyst; (b) temporal N_2, NH_3 and NO_2 effluent concentrations during a lean-rich cycle at 300 °C.

obtained by scraping the washcoat off an LNT1 monolith. Fig. 8a describes the NO conversion and product selectivity at various temperatures. Surprisingly, the NO conversion for the mixed washcoat catalyst was lower than that of both the LNT and dual-layer catalyst. The selectivities of N_2 and N_2O decreased with increasing temperature, while the NO_2 and NH_3 selectivities increased significantly. Fig. 8b shows the effluent N_2, NO_2 and NH_3 during a rich-lean cycle at 300 °C. A large amount of N_2 and NO_2 was produced during the lean phase and NH_3 release while some N_2 formed during the rich phase. The poor performance of the mixed washcoat catalyst is clearly attributed to NH_3 oxidation by O_2. The results cannot be explained by the formation of ammonia nitrate (or nitrite) at low temperatures. If these reactions occurred, much more N_2O than NO_2 would have been observed; see reactions R5, R6, and R9 above. That NO_2 is the main product for $T > 250$ °C is a strong evidence for both NH_3 and NO oxidation. The working concept of the segregated dual layer catalyst is that NH_3 stored in the SCR layer reacts with NO_x that diffuses from the underlying LNT layer or from the bulk gas during the subsequent storage step. Thus, unreacted NO_x is able to react with NH_3 in the presence of excess O_2; i.e. standard SCR reaction. In contrast, on the mixed washcoat catalyst NH_3 that is produced during the rich feed reacts less selectively with O_2 on the highly active PGM sites during the storage step. Apparently, the mixed washcoat catalyst does not effectively utilize NH_3 for stored NO_x regeneration and N_2 formation. While NO_x reduction to N_2, N_2O, and NH_3 occurs during the rich phase, the NH_3 is consumed by O_2 before it can be trapped and react with NO and O_2. The poor utilization of NH_3 decreases the overall NO_x conversion. This oxidation rate increases at high temperatures for both reactions, although the reverse reaction of NO oxidation becomes important above 350 °C. This explanation agrees with the observation that NO_2 selectivity increases at high feed temperatures. Other researchers [41,42] reported that LNT–SCR mixture powder catalyst had a better deNOx performance than LNT catalyst alone. The cause for the disagreement with the previous studies remains unknown. We cannot rule out the possibility that the preparation of the mixed slurry containing the LNT and SCR catalysts may have led to some leaching of Barium from the LNT. In conclusion, the mixed catalyst was not studied any further due to its inferior performance to that of the dual-layer catalyst.

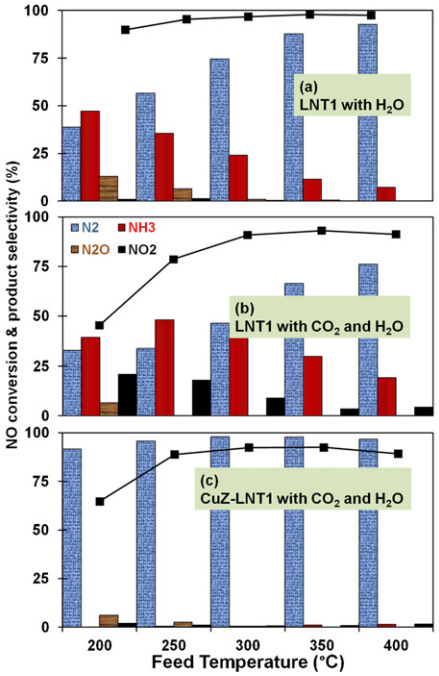

Fig. 9. (a) Performance of LNT1 catalyst with 2.5% H_2O in the feed; (b) performance of LNT1 catalyst with 2.5% H_2O and 2.0% CO_2 in the feed; (c) performance of CuZ–LNT1 catalyst with 2.5% H_2O and 2.0% CO_2 in the feed. Feed temperature was higher than 200 °C to avoid the water condensation.

3.2. *Impact of H_2O and CO_2*

A gas mixture containing 2.5% H_2O and/or 2.0% CO_2 was used in subsequent experiments in order to evaluate the catalyst performance in the presence of these combustion products. Fig. 9a–c shows the NO conversion and product selectivity for temperatures from 200 to 400 °C of LNT1 with a feed to which containing either H_2O or both CO_2 and H_2O, and Cu-zeolite coated LNT1 with a feed

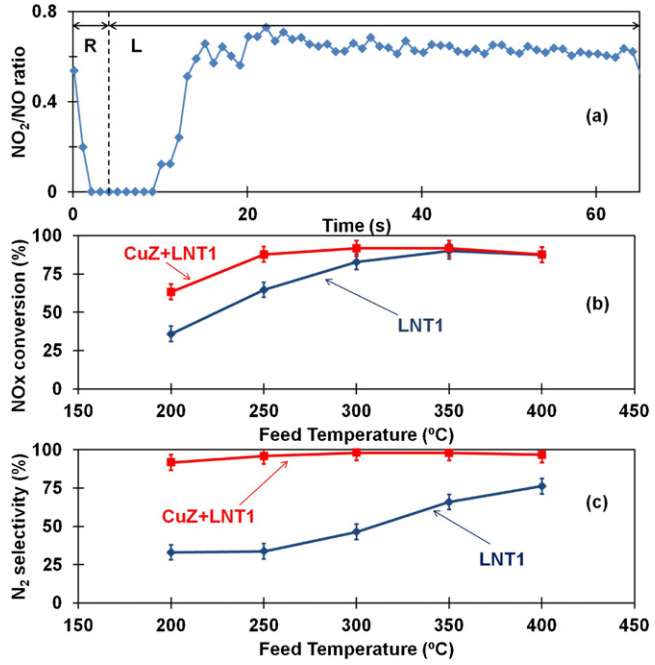

Fig. 10. (a) average NO_2/NO ratio during a lean-rich cycle over LNT1 catalyst at 250 °C; (b) comparison of NO_x conversion of LNT1 and CuZ–LNT1 catalysts; (c) comparison of N_2 selectivity of LNT1 and CuZ–LNT1 catalysts.

containing both H_2O and CO_2. Experiments with feed temperatures lower than 200 °C were not conducted to avoid experimental complications by water adsorption and condensation.

Fig. 9a describes the dependence of NO_x conversion and product selectivity on the temperature for a feed containing 2.5% H_2O. The NO_x conversion increased with temperature up to 350 °C and then very slightly decreased at 400 °C. The N_2 selectivity increased with temperature, while NH_3, N_2O and NO_2 selectivity decreased. Compared to Fig. 3a, NO conversion decreased by only 2–3% upon the H_2O addition. The NH_3 and N_2O selectivity increased by 2–8% at the expense of a 2–10% decrease in the N_2 selectivity. Hence, H_2O addition had a small but adverse influence on NO_x conversion, and changed the product selectivity to a moderate extent.

The dependence of NO_x conversion and product selectivity on the feed temperature for a feed containing of 2.5% H_2O and 2.0% CO_2 is shown in Fig. 9b. Adding CO_2 led to a much larger decrease in the NO conversion than H_2O alone, especially at low temperatures; e.g. 45% decrease at 200 °C compared to the case without CO_2. The N_2 selectivity increased with the increasing temperature while the NH_3 and NO_2 decreased. N_2O only appeared at 200 °C.

The formation of $BaCO_3$ in the presence of CO_2 degrades the performance of the LNT catalyst. Some NO_x storage sites are occupied by CO_2 and thus higher NO and NO_2 slippage occurs during the lean feed. The NO_2/NO ratio during a lean-rich cycle at 250 °C is shown in Fig. 10a. The formed $BaCO_3$ has a higher thermal stability than that of barium nitrates [6,8–11] and this higher stability adversely affects the product selectivity. As reported by Lindholm et al. [10], $BaCO_3$ inhibits the N_2 formation through reactions between nitrates and NH_3. This results in a lower N_2 selectivity and a higher NH_3 selectivity. Another reason for the higher NH_3 selectivity is the accumulation of $BaCO_3$ around the PGM crystallites. Under this condition, the in situ H_2: NO_x ratio is higher which favors NH_3 formation. The deeper regeneration also avoids the N_2O formation.

The dual-layer catalyst performance for a feed containing CO_2 and H_2O is better than that for the LNT alone, as shown in Fig. 9c. The NO conversion and N_2 selectivity increased with temperature up to 350 °C and then decreased slightly at 400 °C. The N_2O selectivity decreased with temperature. A minute NH_3 release was observed above 350 °C. Fig. 10b and c compare the NO_x conversion and N_2 selectivity of the CuZ–LNT1 dual-layer catalyst and the LNT1 catalyst. Considering the large amount of NO_2 generated (Fig. 10a), the NO_x (rather than NO) conversion is reported here. The dual-layer catalyst had a higher NO_x conversion below 300 °C, and was essentially equivalent to that of the LNT1 catalyst above 300 °C. The dual-layer catalyst had a higher N_2 selectivity than LNT1 catalyst over the entire temperature range.

Different NO_x reduction mechanisms account for the differences between the LNT and dual-layer catalysts. On the LNT catalyst, gaseous NO_x needs to be stored as nitrates and/or nitrites before reduction. In contrast, for the dual-layer catalyst, gaseous NO_x can be reduced by trapped NH_3 in the SCR layer in addition to being stored on the LNT layer. Hence, the dependence on the NO_x storage activity of the LNT is weaker. In the presence of CO_2 and H_2O, the LNT1 layer serves as an NH_3 generator during the rich feed (Fig. 9b) and an NO_2 producer during the lean feed (Fig. 10a). The SCR catalyst captures the NH_3 produced during the rich feed and uses it to carry out the SCR reactions during the lean feed at a NO_2/NO ratio of 0.6–0.8, which is in the range for fast SCR reaction [20,21,24,27]. Complete utilization of NO_2 and NH_3 leads to a higher N_2 selectivity from 200 °C to 400 °C and a higher NO_x conversion than that of an LNT catalyst below 300 °C. However, the rate of NH_3 oxidation by O_2 to NO_x is intensified above 300 °C and thus the dual-layer catalyst has about the same NO_x conversion as the LNT catalyst at high temperatures.

3.3. Impact of ceria on LNT and LNT/SCR catalysts

Two LNT catalysts with different ceria loadings of 17 wt% (LNT2) and 34 wt% (LNT3), were prepared. The temperature dependence of the NO conversion and product selectivity of the LNT2 and LNT3 and the Cu-zeolite coated LNT2 and LNT3 catalysts are shown in Fig. 11(a–d).

The performance of both the ceria-containing LNT2 and LNT3 catalysts is similar to that of the barium-only LNT1 catalyst over the temperature range for which N_2, N_2O, NH_3, NO_2 are obtained (Figs. 3a and 11a,c). According to Fig. 11a and c, the cycle-averaged NO conversion and N_2 selectivity increased as the temperature increased, while the N_2O selectivity decreased. The maximum cycle-averaged NH_3 selectivity of about 75% was achieved at 150 °C. At the same temperature, the NO conversion of the ceria-containing LNT catalysts was higher than the ceria-free LNT1 sample. The primary product was NH_3 below 250 °C and N_2 above 250 °C.

The addition of ceria affects some subtle features of the NO conversion and product distribution. First, the cycle-averaged NO conversion and NH_3 yield (product of NO conversion and NH_3 selectivity) are higher below 250 °C. The is due to an increase in the NO_x storage capacity as the ceria provides new storage sites in addition to those already existing on the BaO. This is proven in Fig. 12a, which compares the NO_x storage of the LNT1, LNT2, and LNT3 catalysts. This increase in NO_x storage increases the amount of NO_x available for reduction and increases the NO conversion and the NH_3 yield. Since ceria-based nitrates have lower stability than barium-based nitrates, an easier reduction can be achieved at low temperatures [1,46]. A second feature is an increase in the N_2 selectivity and decrease in the NH_3 yield above 250 °C. At these high temperatures, ceria increases the NH_3 oxidation rate due to its oxygen storage capacity and oxidation activity [45]. Moreover, NH_3 oxidation has a high selectivity toward N_2 [6].

The increased NO conversion at low temperatures by ceria addition provides a way to reduce the requisite PGM loading. As shown in Figs. 3a, 11a and 11c, the NO conversion obtained at low-temperatures is much lower than the conversion obtained at high

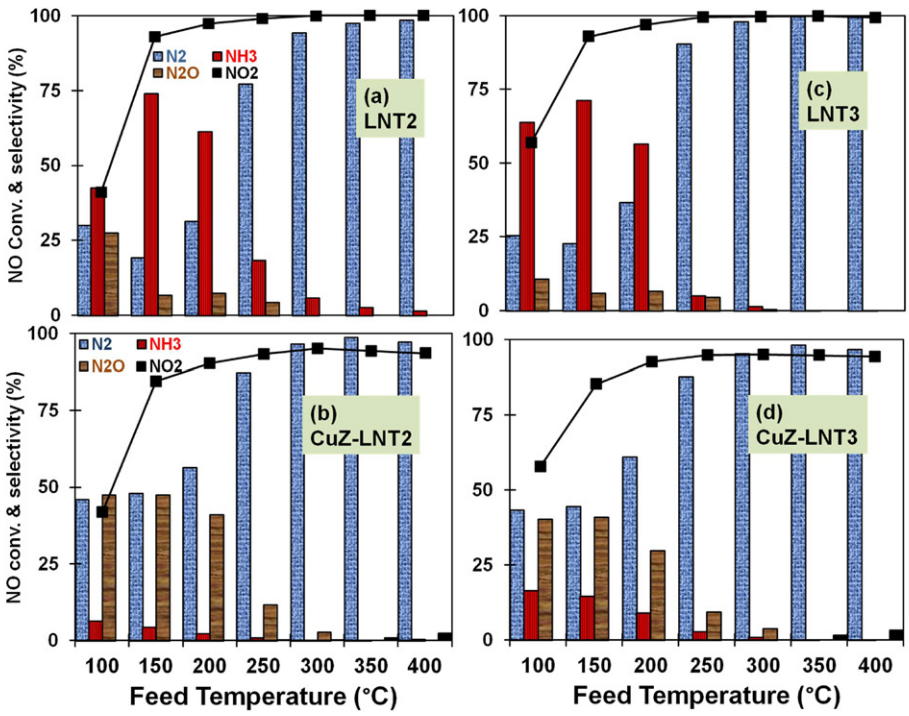

Fig. 11. Performance of (a) LNT2 catalyst; (b) CuZ–LNT2 dual layer catalyst; (c) LNT3 catalyst; (d) CuZ–LNT3 dual layer catalyst.

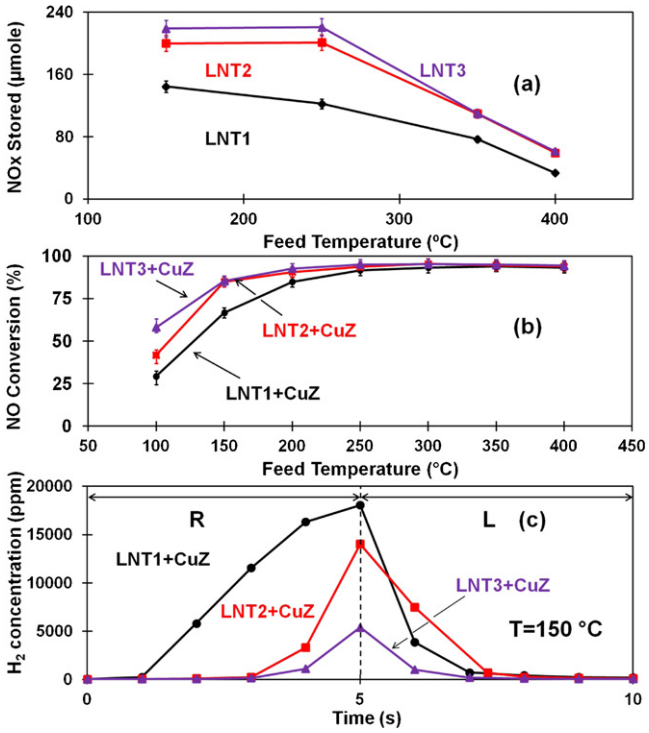

Fig. 12. (a) NO_x storage capacity of LNT1, LNT2 and LNT3; (b) comparison of NO conversions of three dual layer catalysts; (c) the average H_2 effluents in CuZ coated LNT1, LNT2 and LNT3 catalysts at 150 °C during a lean-rich cycle.

temperatures. Thus, the low temperature performance dictates the amount of PGM needed to achieve a prescribed level of NO_x conversion. That is, the largest amount of PGM necessary to achieve a desired NO conversion over the anticipated range of typical operating temperatures; i.e. 150–400 °C, is at the lowest temperature. The surplus PGM over that needed at the high temperatures is needed to achieve the same specified conversion at the lowest temperature. In the presence of ceria, the low-temperature NO conversion is increased significantly. Thus, the PGM loading in a ceria-containing LNT can be reduced without comprising NO conversion at low temperatures and minimizing the excess PGM at high temperatures.

A Cu/ZSM5 layer was coated on the top of the ceria-containing LNT2 and LNT3 catalysts. Fig. 11b and d show the NO conversion and product selectivity for the dual-layer CuZ/LNT2 and CuZ/LNT3 catalysts, respectively. NO conversion increased with temperature up to 300 °C and then slightly decreased. N_2 selectivity increased with temperature, while N_2O exhibited an opposite trend. NH_3 slip increased as temperature decreased. Some NO_2 was observed above 350 °C. The trends of NO conversion and product selectivity are comparable to those of the Cu-zeolite coated LNT1 shown in Fig. 3b. For a more convenient comparison, the NO conversions from the three dual-layer catalysts are summarized in Fig. 12b. Clearly, the ceria containing dual-layer catalysts lead to higher NO conversion, especially at low temperatures. Again, the main reason is the increased NO_x storage (Fig. 12a) and the reduced stored nitrate stability.

The addition of ceria impacts among others the N_2 selectivity and NH_3 slip which exceed the values obtained by the barium-only dual-layer catalyst at low temperatures. The regeneration of stored NO_x in the presence of ceria increases the N_2 selectivity and decreases the N_2O selectivity. The enhanced NH_3 formation by the ceria-containing dual-layer catalysts is the opposite of that when using a series of monolith bricks [32]. That is, for high loading of OSC (oxygen storage component) NH_3 oxidation is enhanced and thus the NH_3 yield decreases. However, the situation at low temperature is due to the enhancement by ceria of the low-temperature reduction of stored NO_x. As shown in Fig. 12c, the hydrogen conversion increases with the ceria loading in dual-layer catalysts. At 150 °C, CuZ–LNT1 leads to an 8% hydrogen conversion, CuZ–LNT2–23% and CuZ–LNT3–49%. The addition of ceria to LNT catalysts increases the H_2 conversion due to two effects. First, the ceria increases the NO_x and oxygen storage on the catalyst. The barium-only LNT1 has a

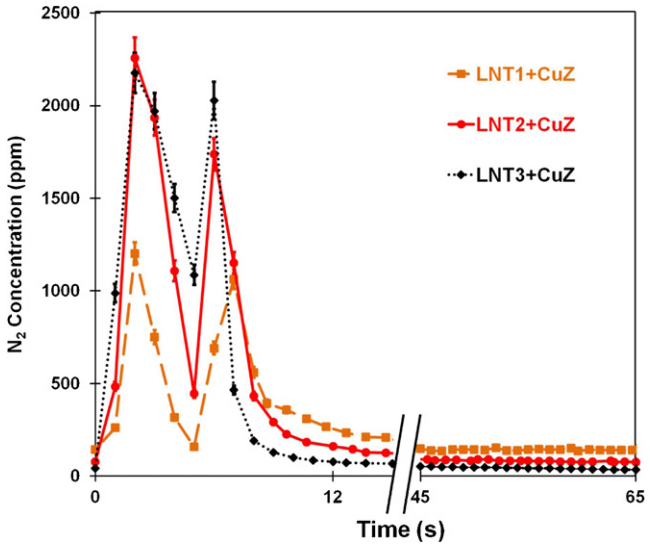

Fig. 13. Comparison of N_2 effluent from three dual layer catalysts. LNT1 + CuZ is the dashed line; LNT2 + CuZ is the solid line; LNT3 + CuZ is the dotted line.

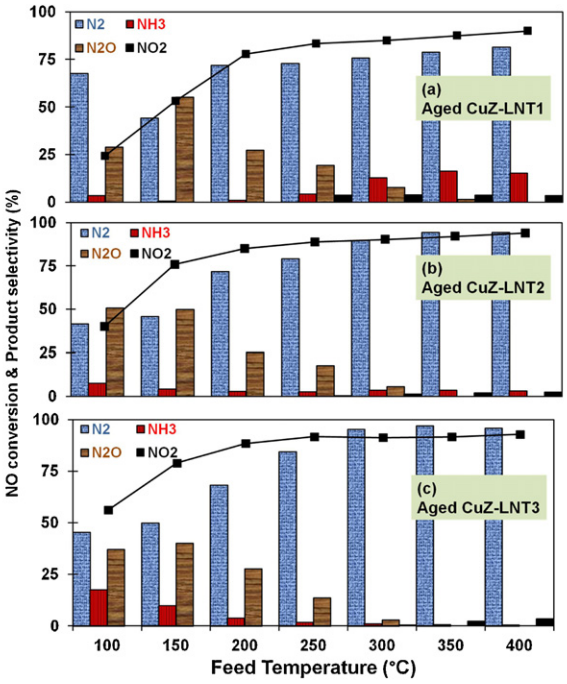

Fig. 14. Performance of (a) aged CuZ–LNT1 multilayer catalyst; (b) aged CuZ–LNT2 multilayer catalyst; (c) aged CuZ–LNT3 multilayer catalyst.

lower capacity for NO_x and oxygen storage than LNT2 and LNT3. Second, the low-temperature PGM activity is enhanced by the ceria addition [45]. That is, ceria-containing LNT catalysts have a higher, low-temperature regeneration activity than the barium-only catalyst. Better utilization of the feed H_2 generates more NH_3 during the regeneration and more storage sites after the regeneration. In addition, the generated NH_3 is captured by the SCR layer instead of being consumed by the ceria in the LNT layer downstream. The Cu zeolite top layer does not have the capacity to store all the large amount of NH_3 produced. On the other hand, the addition of ceria increases the rate of NH_3 oxidation. As shown by Fig. 7, the apparent reaction order of NH_3 oxidation increases from 0.46 to 0.68 with an increase of ceria loading in the LNT catalyst. The intensified oxidation consumes more trapped NH_3 in the dual-layer catalysts. Thus, less NH_3 is available for the SCR reactions. Fig. 13 shows the N_2 effluents from the three dual-layer catalysts at 300 °C. The amount of N_2 formed was similar for the three dual-layer catalysts with 9.6, 10.2 and 10.1 μmole for CuZ–LNT1, CuZ–LNT2 and CuZ–LNT3, respectively. The ceria-containing dual-layer catalysts generated higher N_2 peaks than the one that does not contain ceria during both the lean and rich feeds. The amount of N_2 generated continuously after the first 3–5 s of the switch to the lean feed decreases with the increase of ceria loading. This indicates that ceria addition increases the rate of NH_3 oxidation, which decreases the rate of the desired SCR reactions.

An adjustment of the SCR: LNT loading ratio in the washcoat and the amount of ceria added to the LNT are essential to maximize the NH_3 utilization. The main task of the dual-layer catalyst is NO_x reduction. Thus, at low-temperatures (<250 °C), high ceria loading is favorable due to the increased NO_x storage capacity and its synergy with PGM for NH_3 generation. Its addition enables a reduction of the amount of PGM on the LNT catalyst. The NO_x reduction depends more on the relatively inexpensive SCR rather than the expensive LNT. On the other hand, at high-temperatures (>250 °C) the NO_x reduction favors a low ceria loading in dual-layer catalysts to avoid the undesired NH_3 oxidation. These issues are currently being explored and will be reported in a future publication.

3.4. Dual-layer catalyst durability

Hydrothermal aging deactivates LNT catalysts due to an increase in the PGM particle size (sintering), and resulting reduction in the interface between the PGM and barium storage phase [52,53]. In the absence of ceria, aging of LNT catalysts leads to an increase the selective production of ammonia and decreases the overall storage and reduction. On the other hand, the SCR catalyst is deactivated by hydrothermal aging due to dealumination and the decreased oxidation activity of the Cu zeolite [57–59]. (Remark: the addition of Mn to SCR catalyst is known to improve the SCR catalyst durability and low-temperature activity [60,61]. This is a subject of on-going research in our group.) This leads to a decrease in the ammonia storage capacity and an increase in the NH_3 slip, assuming the supply of ammonia from the LNT is fixed. The impact of ceria loading on the NH_3 selectivity is undoubtedly affected by the decrease of the ceria surface area and the NO_x storage capacity during aging [54–56]. In summary, the effect of aging on the LNT/SCR catalyst performance is complicated by the effects of several trends. The decreased NO conversion upon hydrothermal aging of the dual-layer catalysts is due to the deactivation of both the LNT and SCR catalysts.

Hydrothermal aging and SEM–EDS experiments were conducted to understand the durability and quantify the effect of aging on the dual-layer catalyst. Fig. 14a–c describes NO conversion and product selectivity of the three aged dual-layer catalysts for different feed temperatures. For all three LNT catalysts, NO conversion and N_2 selectivity increased with temperature. NH_3 slip from the barium-only LNT1 increased with temperature, while the opposite trend was observed in the ceria-containing LNT2 and LNT3 catalysts. N_2O was mainly produced from 100 to 250 °C for all three catalysts.

Fig. 15a compares the NO conversion of fresh catalysts (solid line) with that of aged ones (dashed lines). The NO conversions of the aged dual-layer catalysts are lower than those of the fresh ones for all feed temperatures. The difference in NO conversion between the fresh and aged catalysts decreases upon an increase of the ceria loading in the LNT layer. The deactivation is largest for barium-only dual-layer catalyst. The NO conversion decreased by 12.6% at 150 °C for the Cu-zeolite coated LNT1 dual-layer catalyst. These results suggest that the stability of the barium-containing dual-layer catalyst may be enhanced by the addition of ceria.

Fig. 15b shows the effect of aging on the ammonia selectivity. The trends are rather complex. In the absence of ceria, the ammonia

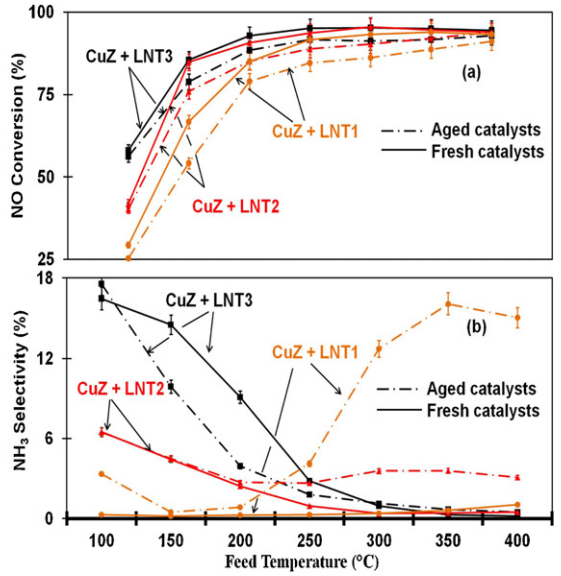

Fig. 15. (a) Comparison of NO conversion of aged and fresh multilayer catalysts; (b) comparison of NH_3 selectivity of aged and fresh multilayer catalysts.

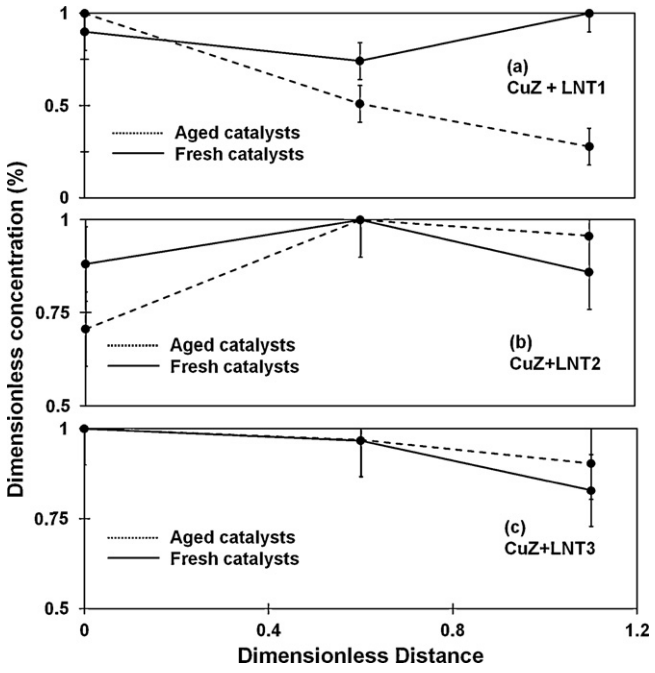

Fig. 16. Profile of Pt concentration in the washcoats. Concentrations are normalized by the maximum value of each sample. Solid lines are for fresh catalysts; dashed lines are for aged catalysts. The dimensionless distance 1.0 = 60–67 μm. According to our last discussion, only metal concentration in LNT layer is shown in this figure and the dimensionless distance 1.2 refers to the interface.

selectivity increases dramatically with aging, especially at high temperatures. A comparison of the two ceria-containing catalysts shows trends similar to those of the ceria-free catalyst, but not as dramatic. That is, at higher temperature the ammonia selectivity is higher for the aged than fresh catalyst. For the catalyst with the highest loading of ceria, the aging results in a decrease in the ammonia selectivity, for temperatures below 300 °C. This could be a result of a decrease in the ceria surface area and a corresponding decrease in the NO_x storage. Additional experiments are needed to elucidate these trends.

We studied the impact of the hydrothermal aging on the profile of the Ce, Ba and Pt elements in the washcoat. Fig. 16a–c shows the normalized Pt concentration profiles versus the dimensionless position. A dimensionless coordinate was used to enable a direct comparison among the three dual-layer catalysts, which have somewhat different washcoat thicknesses. As the thickness of the LNT layer is about 1.5 that of the SCR (indicated in Fig. 1), we refer to the total washcoat thickness as 2.0 and the interface between the LNT and SCR as 1.2. In Fig. 16a, the Pt concentration in the LNT layer decreased after aging. The PGM migration may lower NO conversion due to intensified NH_3 oxidation and the separation between PGM and barium. On the other hand, in the ceria-added catalysts the change in Pt element concentrations before and after hydrothermal aging were less pronounced (Fig. 16b and c). Although the barium profile is not shown in the figures, its trend is similar to those of the Pt. In the absence of ceria, the barium concentration in LNT and SCR layers became uniform after aging. That indicates that some barium migrated from the LNT layer to the SCR layer. Ceria mitigated barium migration from the LNT to the SCR in the dual-layer catalyst. The experiments reveal that ceria addition improves the structural stability of the dual-layer catalysts.

4. Concluding remarks

In this study, the behaviors of SCR-top LNT dual-layer catalysts during lean-rich cycles were studied in the temperature range from 100 °C to 400 °C. The main behavioral features of dual layers catalysts for combined NSR and SCR are:

- Dual-layer catalyst capture NH_3 generated from LNT layer and use it for SCR reactions. As a result, N_2 selectivity can be increased.
- NH_3 oxidation to NO_x lowers the NO conversion of dual-layer catalyst. This is especially problematic at high temperatures.
- In the presence of CO_2 and H_2O, dual-layer catalyst utilizes well the formed NO_2 and NH_3 for SCR reactions. Hence, dual-layer catalyst has a higher NO_x conversion from 200 to 300 °C and a higher N_2 selectivity than LNT catalyst over the whole temperature range
- The addition of ceria leads to a high NO_x storage capacity and efficient regeneration at low temperatures. The PGM loading in the ceria containing LNT catalyst can be lower than in the barium-only one. The NH_3 formation at low temperatures increases with a ceria loading increase. However, ceria enhances the NH_3 oxidation at high temperatures.
- The ceria-contained dual-layer catalysts have a higher resistance toward hydrothermal aging than the barium-only one. PGM and barium migration is mitigated by the presence of ceria.

These findings show that the dual-layer catalyst can reduce NO_x emission below 300 °C, especially in the presence of CO_2 and H_2O. Ceria loading is an important catalyst design variable for low-temperature performance and catalyst durability. The NH_3 formation is enhanced by ceria at low temperatures and NO_x reduction depends more on the SCR catalyst. As a result, PGM loading can be reduced. Ceria-promoted H_2 generation via the water–gas-shift reaction with subsequent NH_3 generation is currently under investigation. The optimization of other catalyst design variables, such as the ceria loading and SCR layer thickness, and the impact of operating conditions, such as the lean-rich cycle time and the inclusion of SO_x [62,63], are the subjects of ongoing research. This new knowledge will enable a determination which catalyst configuration multi-brick or dual-layer provides superior performance.

Acknowledgements

This study was funded by grants from the U.S. DOE National Energy Technology Laboratory as part of the Vehicles Technologies

Program (DE-EE0000205). We would like to thank BASF (Iselin, NJ) for the supply of LNT catalysts.

References

[1] Y. Ji, J.S. Choi, T.J. Toops, M. Crocker, M. Naseri, Catalysis Today 136 (2008) 146–155.
[2] T. Morita, N., Suzuki, N., Satoh, K., Wada, H. Ohno, SAE 2007-01-0239.
[3] K. Wada, N., Suzuki, N., Satoh, T., Morita, S., Yamaguchi, H. Ohno, SAE 2007-01-1933.
[4] M. Hatanaka, N. Takahashi, T. Tanabe, Y. Nagai, K. Dohmae, Y. Aoki, T. Yoshida, H. Shinjoh, Applied Catalysis B: Environmental 99 (2010) 336–342.
[5] J.H. Kwak, D.H. Kim, J. Szanyi, C.H.F. Peden, Applied Catalysis B: Environmental 84 (2008) 545–551.
[6] Y.J. Ren, M.P. Harold, ACS Catalysis 1 (2011) 969–988.
[7] S.S. Mulla, N. Chen, L. Cummaranatunge, W.N. Delgass, W.S. Epling, F.H. Ribeiro, Catalysis Today 114 (2006) 57–63.
[8] L. Lietti, I. Nova, P. Forzatti, Journal of Catalysis 257 (2008) 270–282.
[9] F. Frola, F. Prinetto, G. Ghiotti, L. Castoldi, I. Nova, L. Lietti, P. Forzatti, Catalysis Today 126 (2007) 81–89.
[10] A. Lindholm, N.W. Currier, E. Fridell, A. Yezerets, L. Olsson, Applied Catalysis B: Environmental 75 (2007) 78–87.
[11] I. Nova, L. Lietti, P. Forzatti, F. Prinetto, G. Ghiotti, Catalysis Today 151 (2010) 330–337.
[12] S.S. Mulla, S.S. Chaugule, A. Yezerets, N.W. Currier, W.N. Delgass, F.H. Ribeiro, Catalysis Today 136 (2008) 136–145.
[13] J. Wang, Y. Ji, V. Easterling, M. Crocker, M. Dearth, R.W. McCabe, Catalysis Today 175 (2011) 83–92.
[14] R.D. Clayton, M.P. Harold, V. Balakotaiah, Applied Catalysis B: Environmental 84 (2008) 616–630.
[15] R.D. Clayton, M.P. Harold, V. Balakotaiah, Applied Catalysis B: Environmental 81 (2008) 161–181.
[16] R.D. Clayton, M.P. Harold, V. Balakotaiah, C.Z. Wan, Applied Catalysis B: Environmental 90 (2009) 662–676.
[17] D. Bhatia, M.P. Harold, V. Balakotaiah, Catalysis Today 151 (2010) 314–329.
[18] J.Y. Luo, W.S. Epling, Applied Catalysis B: Environmental 97 (2010) 236–247.
[19] B. Shakya, M.P. Harold, V. Balakotaiah, Catalysis Today (2012), http://dx.doi.org/10.1016/j.cattod.2012.01.037.
[20] M. Paule, A., Mackensen, R., Binz, C. Enderle, SAE 2011-01-0294.
[21] N. Waldbuesser, J., Guenther, H., Hoffmann, O., Erlenmayer, F., Duvinage, C., Enderle, J., Schommers, D. Waeller, SAE 2011-01-1172.
[22] M. Colombo, I. Nova, E. Tronconi, Catalysis Today 151 (2010) 223–230.
[23] J.M. Fedeyko, B. Chen, H.Y. Chen, Catalysis Today 151 (2010) 231–236.
[24] P.S. Metkar, N. Salazar, R. Muncrief, V. Balakotaiah, M.P. Harold, Applied Catalysis B: Environmental 104 (2011) 110–126.
[25] K. Kamasamudram, N.W. Currier, X. Chen, A. Yezerets, Catalysis Today 151 (2010) 212–222.
[26] K. Kamasamudram, N.W., Currier, T., Szailer, A. Yezerets, SAE 2010-01-1182.
[27] P.S. Metkar, V. Balakotaiah, M.P. Harold, Applied Catalysis B: Environmental 111–112 (2012) 67–80.
[28] H.S. Gandhi, J.V. Cavataio, R.H. Hammerle, Y.S. Cheng, US Patent 7485273.
[29] H.S. Gandhi, J.V. Cavataio, R.H. Hammerle, Y.S. Cheng, US Patent 7674743.
[30] L. Xu, R. McCabe, P. Tennison, H.W. Jen, SAE 2011-01-0308.
[31] F. Rohr, I. Grißtede, A. Sundararajan, W. Müller, SAE 2008-01-0766.
[32] H.Y. Chen, E.C. Weigert, J.M. Fedeyko, J.P. Cox, P.J. Andersen, SAE 2010-01-0302.
[33] J.E. McCarthy, Jr., E. Dykes, E. Ngan, SAE 2010-01-1942.
[34] J.R. Theis, J.A. Ura, J.J. Li, G.G. Surnilla, J.M. Roth, C.T. Goralski Jr., SAE 2003-01-1159.
[35] A. Lindholm, H. Sjövall, L. Olsson, Applied Catalysis B: Environmental 98 (2010) 112–121.
[36] B. Pereda-Ayo, D. Duraiswami, J.R. González-Velasco, Catalysis Today 172 (2011) 66–72.
[37] C.K. Seo, H. Kim, B. Choi, M.T. Lim, Journal of Industrial Engineering and Chemistry 17 (2011) 382–385.
[38] C.K. Seo, H. Kim, B. Choi, M.T. Lim, C.H. Lee, C.B. Lee, Catalysis Today 164 (2011) 507–514.
[39] R. Bonzi, L. Lietti, L. Castoldi, P. Forzatti, Catalysis Today 151 (2010) 376–385.
[40] P. Forzatti, L. Lietti, Catalysis Today 155 (2010) 131–139.
[41] L. Castoldi, R. Bonzi, L. Lietti, P. Forzatti, S. Morandi, G. Ghiotti, S. Dzwigaj, Journal of Catalysis 282 (2011) 128–144.
[42] E.C. Corbos, M. Haneda, X. Courtois, P. Marecot, D. Duprez, H. Hamada, Applied Catalysis A-General 365 (2009) 187–193.
[43] T. Nakatsuji, M. Matsubara, J. Rouistenmaki, N. Sato, H. Ohno, Applied Catalysis B: Environmental 77 (2007) 190–201.
[44] D. Bhatia, R.W. McCabe, M.P. Harold, V. Balakotaiah, Journal of Catalysis 266 (2009) 106–119.
[45] Y. Liu, M.P. Harold, D. Luss, Applied Catalysis A-General 397 (2011) 35–45.
[46] Y. Ji, V. Easterling, U. Graham, C. Fisk, M. Crocker, J.S. Choi, Applied Catalysis B: Environmental 103 (2011) 413–427.
[47] R.D. Clayton, M.P. Harold, V. Balakotaiah, AIChE Journal 55 (2009) 687–700.
[48] K. Su, H. Xia, E. Hensen, R. van Santen, C. Li, Journal of Catalysis 238 (2006) 186–195.
[49] M.H. Groothaert, K. Lievens, H. Leeman, B.W. Weckhuysen, R.A. Schoonheydt, Journal of Catalysis 220 (2003) 500–512.
[50] X. Zhang, Q. Shen, C. He, C. Ma, J. Cheng, L. Li, Z. Hao, ACS Catalysis 2 (2012) 512–520.
[51] A. Grossale, I. Nova, E. Tronconi, D. Chatterjee, M. Weibel, Journal of Catalysis 256 (2008) 312–322.
[52] Y. Ji, V. Easterling, U. Graham, C. Fisk, M. Crocker, J. Choi, Applied Catalysis B: Environmental 103 (2011) 413–427.
[53] T.J. Toops, B.G. Bunting, K. Nguyen, A. Gopinath, Catalysis Today 123 (2007) 285–292.
[54] N. Wilken, K. Wijayanti, K. Kamasamudram, N.W. Currier, R. Vedaiyan, A. Yezerets, L. Olsson, Applied Catalysis B: Environmental 111–112 (2012) 58–66.
[55] T.J. Toops, K. Nguyen, A.L. Foster, B.G. Bunting, N.A. Ottinger, J.A. Pihl, E.W. Hagaman, J. Jiao, Catalysis Today 151 (2010) 257–265.
[56] Y. Cheng, J. Hoard, C. Lambert, J.H. Kwak, C.H.F. Peden, Catalysis Today 136 (2008) 34–39.
[57] E. Rogemond, R. Fréty, V. Perrichon, M. Primet, M. Chevrier, C. Gauthier, F. Mathis, Applied Catalysis A-General 156 (1997) 253–265.
[58] Y. Nagai, K. Dohmae, Y. Ikeda, N. Takagi, N. Hara, T. Tanabe, G. Guilera, S. Pascarelli, M.A. Newton, N. Takahashi, H. Shinjoh, S. Matsumoto, Catalysis Today 175 (2011) 133–140.
[59] V. Easterling, Y. Ji, M. Crocker, J. Ura, J.R. Theis, R.W. McCabe, Catalysis Today 151 (2010) 338–346.
[60] P.G. Smirniotis, D.A. Pena, B.S. Uphade, Angewandte Chemie-International Edition in English 40 (2001) 2479–2482.
[61] G. Qi, R.T. Yang, R. Chang, Applied Catalysis B: Environmental 51 (2004) 93–106.
[62] R. Burch, J.P. Breen, F.C. Meunier, Applied Catalysis B: Environmental 39 (2002) 283–303.
[63] A. Takami, T. Takemoto, H. Iwakuni, K. Yamada, M. Shigetsu, K. Komatsu, Catalysis Today 35 (1997) 75–81.